CZECH TECHNICAL UNIVERSITY IN PRAGUE

Faculty of Electrical Engineering

BACHELOR THESIS

Roman Sushkov

Self-Organizing Structures for the Travelling Salesman Problem in a Polygonal Domain

Department of Cybernetics

Thesis supervisor: **RNDr. Miroslav Kulich, Ph.D.**

České vysoké učení technické v Praze
Fakulta elektrotechnická

Katedra kybernetiky

ZADÁNÍ BAKALÁŘSKÉ PRÁCE

Student:	Roman S u s h k o v
Studijní program:	Kybernetika a robotika (bakalářský)
Obor:	Robotika
Název tématu:	Samoorganizující se struktury pro problém obchodního cestujícího v polygonální doméně

Pokyny pro vypracování:

1. Seznamte se s metodami samoorganizujících se struktur pro problém obchodního cestujícího [1,2,3].
2. Naimplementujte výše zmíněné metody. Pro vizualizaci vývoje metod použijte knihovnu VTK.
3. Použijte vybranou metodu vícedimenzionálního škálování pro rozšíření metod tak, aby pracovaly v prostředí s polygonálními překážkami.
4. Experimentálně ověřte funkčnost a vlastnosti (zejména kvalitu řešení a výpočetní náročnost algoritmů) implementovaných metod.

Seznam odborné literatury:

[1] E. M. Cochrane and J. E. Beasley: The co-adaptive neural network approach to the Euclidean travelling salesman problem. Neural Netw. 16, 10 (December 2003), 1499-1525.
[2] J. Zhang, X. Feng, B. Zhou, and D. Ren: An overall-regional competitive self-organizing map neural network for the Euclidean traveling salesman problem. Neurocomput. 89 (July 2012), 1-11.
[3] S. Somhom , A. Modares, T. Enkawa: A self-organising model for the travelling salesman problem. Journal of the Operational Research Society, 1997, 48 (9): 919-928.
[4] Ch. Faloutsos and King-Ip Lin: FastMap: a fast algorithm for indexing, data-mining and visualization of traditional and multimedia datasets. *SIGMOD Rec.* 24, 2 (May 1995), 163-174.
[5] A, Elad, R. Kimmel: On bending invariant signatures for surfaces, Pattern Analysis and Machine Intelligence, IEEE Transactions on , vol.25, no.10, pp.1285,1295, Oct. 2003.

Vedoucí bakalářské práce: RNDr. Miroslav Kulich, Ph.D.

Platnost zadání: do konce letního semestru 2015/2016

L.S.

doc. Dr. Ing. Jan Kybic	prof. Ing. Pavel Ripka, CSc.
vedoucí katedry	**děkan**

V Praze dne 28. 1. 2015

Czech Technical University in Prague
Faculty of Electrical Engineering

Department of Cybernetics

BACHELOR PROJECT ASSIGNMENT

Student:	Roman S u s h k o v
Study programme:	Cybernetics and Robotics
Specialisation:	Robotics
Title of Bachelor Project:	Self-Organizing Structures for the Travelling Salesman Problem in a Polygonal Domain

Guidelines:

1. Get acquainted with self-organizing structures for the Travelling Salesman Problem [1,2,3].
2. Implement the above methods. Utilize the VTK library for visualization of the methods' behavior.
3. Extend the implemented methods for environments with polygonal obstacles by utilizing the chosen method for multi-dimensional scaling.
4. Evaluate experimentally functionality and properties of the implemented methods. Focus mainly on quality of the generated solutions and complexity of the algorithms.

Bibliography/Sources:

[1] E. M. Cochrane and J. E. Beasley: The co-adaptive neural network approach to the Euclidean travelling salesman problem. Neural Netw. 16, 10 (December 2003), 1499-1525.
[2] J. Zhang, X. Feng, B. Zhou, and D. Ren: An overall-regional competitive self-organizing map neural network for the Euclidean traveling salesman problem. Neurocomput. 89 (July 2012), 1-11.
[3] S. Somhom , A. Modares, T. Enkawa: A self-organising model for the travelling salesman problem. Journal of the Operational Research Society, 1997, 48 (9): 919-928.
[4] Ch. Faloutsos and King-Ip Lin: FastMap: a fast algorithm for indexing, data-mining and visualization of traditional and multimedia datasets. *SIGMOD Rec.* 24, 2 (May 1995), 163-174.
[5] A, Elad, R. Kimmel: On bending invariant signatures for surfaces, Pattern Analysis and Machine Intelligence, IEEE Transactions on , vol.25, no.10, pp.1285,1295, Oct. 2003.

Bachelor Project Supervisor: RNDr. Miroslav Kulich, Ph.D.

Valid until: the end of the summer semester of academic year 2015/2016

L.S.

doc. Dr. Ing. Jan Kybic	prof. Ing. Pavel Ripka, CSc.
Head of Department	**Dean**

Prague, January 28, 2015

Declaration

I hereby declare that I have completed this thesis independently and that I have used only the sources (literature, software, etc.) listed in the enclosed bibliography.

In Prague on............................ ....

Prohlášení autora práce

Prohlašuji, že jsem předloženou práci vypracoval samostatně a že jsem uvedl veškeré použité informační zdroje v souladu s Metodickým pokynem o dodržování etických principů při přípravě vysokoškolských závěrečných prací.

V Praze dne............................ ....

Podpis autora práce

Acknowledgements

I wish to express my sincere gratitude to my thesis supervisor RNDr. Miroslav Kulich, Ph.D for his guidance and all his valuable ideas. I would also like to thank my family for supporting me during the thesis preparation.

Access to computing and storage facilities owned by parties and projects contributing to the National Grid Infrastructure MetaCentrum, provided under the programme "Projects of Large Infrastructure for Research, Development, and Innovations" (LM2010005), is greatly appreciated.

Abstrakt

Tato práce se zabývá řešením problému obchodního cestujícího v polygonální doméně samoorganizujícími se strukturami. Hlavní myšlenka spočívá v transformaci polygonální domény do metrického prostoru vyšší dimenze, což umožňuje řešit dotazy na vzdálenost mezi městem a neuronem efektivně. V rámci práce byly implementovány dvě metody multidimenzionálního škálování realizující transformaci prostoru s překážkami a tři typy neuronových sítí pro nalezení řešení problému obchodního cestujícího. Byly otestovány různé parametry implemetovaných metod a jejich vliv na kvalitu výsledného řešení.

Klíčová slova

Samoorganizující se struktury, multidimenzionální škálování, problém obchodního cestujícího, metrický problém obchodního cestujícího.

Abstract

The topic of this study is searching for a solution of the travelling salesman problem in a polygonal domain using the self-organising maps. The main idea is based on the transformation of the polygonal domain into a metric space with a high number of dimensions, which facilitates the distance computation between the guards and the neurons. Two methods of the multidimensional scaling for the transformation of the polygonal domain and three self-organising map algorithms that search for the travelling salesman problem solution were implemented. The implemented methods were tested with various parameters, and the impact of the parameters on the quality of the solution was evaluated.

Keywords

Self-organising maps, multidimensional scaling, metric travelling salesman problem, travelling salesman problem.

Contents

List of Figures

List of Tables

List of algorithms

Chapter 1

Introduction

Travelling salesman problem (TSP) is a classic NP-hard problem. It can be stated as a problem of finding the shortest closed path between a set of cities (guards). Generally, the TSP is a graph problem (guards are represented by the vertices, and the weights of the edges represent distances between the guards). The metric TSP is a special case of the general TSP. In the metric TSP, the guards have coordinates, and the distances can be computed according to the used metric. One of the widely known instance of the metric TSP is the Euclidean TSP, where the Euclidean distance is used. Self-organising maps [1] (SOM) have been used [2][3][4] for solving the Euclidean travelling salesman problem.

Developing fast and reliable algorithms for TSP solving in a polygonal domain is important for mobile robot navigation. Many areas populated by humans can be modelled in a polygonal domain, such as floorplans, parks and streets. It is not necessary to know the optimal tour since the environments are frequently dynamic, so temporary or moving obstacles (such as people) would corrupt the implementation of the optimal tour anyway. Hence, fast heuristics are valuable in such cases.

A method of solving the TSP in a polygonal domain by using self-organising maps is covered in this thesis. Multidimensional scaling (MDS) algorithms are used here to transform a TSP in a polygonal domain into a metric TSP. Two MDS algorithms and three SOM algorithms were chosen for that purpose.

The thesis is structured as follows: in chapter 2 the used approach and the used algorithms are described. In chapter 3 the implementation (including the changes of the used algorithms) is discussed. The experiments and the discussion of the results are covered in chapter 4. Chapter 5 is the conclusion.

Chapter 2

Algorithm description

The algorithm searches for the Travelling Salesman Problem (TSP) solution in a polygonal domain. TSP consists of finding the shortest route that visits all objects (guards) from a given set at least once and returns to the first guard in the list (the input is a set of guards, the output is an order list of the guards). Polygonal domain $\mathcal{S}_o$ is an environment that consists of a two-dimensional map with guards and polygonal boundaries and obstacles.

TSP is an NP-hard problem that can be solved by various approaches. Both heuristic and non-heuristic methods of solving this problem have been developed. The exact solution of the TSP can be found by evaluating all possible tours (all permutations of the set of guards) with computational complexity $O(n!)$, which makes this approach impractical. Other methods that reduce the time complexity have been developed, such as Held–Karp, which is a more sophisticated method of solving the TSP with time complexity $O(n^2 2^n)$. There is also a number of heuristics that produce a solution that is not necessarily optimal. They are important because the optimal solution is not always required in the real-life problems, where the computation speed is more important. These heuristics include: constructive heuristics (greedy algorithm), iterative improvement(k-opt, or Lin-Kernighan heuristics [5]) and randomised improvement(genetic algorithms [6], ant colony optimisation algorithm [7]).

It has been proposed [2][3][4] to use Self-Organising maps [1] (SOM) for the Euclidean TSP and for the TSP in a polygonal domain [8][9]. SOM is a kind of a neural network. Input of that network is the coordinates of a guard. For each input that has been fed into the network neurons change their weights: the winning neuron (the closest) and its neighbours move towards the input. By feeding the guards that have to be visited into the network repeatedly, the neurons converge to a state from which we can find a tour.

The map in Fig. 2.1a is *jari*, which is a floorplan of a real building. 4 guards are shown as the red circles. The neurons (blue circles) initially lie on a small ring. As already mentioned, the guards are repeatedly fed into the neural network. After the current input (the guard marked by a yellow dot in Fig. 2.1) has been fed into the SOM, the neurons reorganise as shown in Fig. 2.1b: the winning neuron (the neuron marked by a yellow dot in Fig. 2.1) and its neighbours

Figure 2.1: SOM learning in $\mathcal{S}_o$. The guard that is used as the input and the winning neuron are marked by yellow dots.

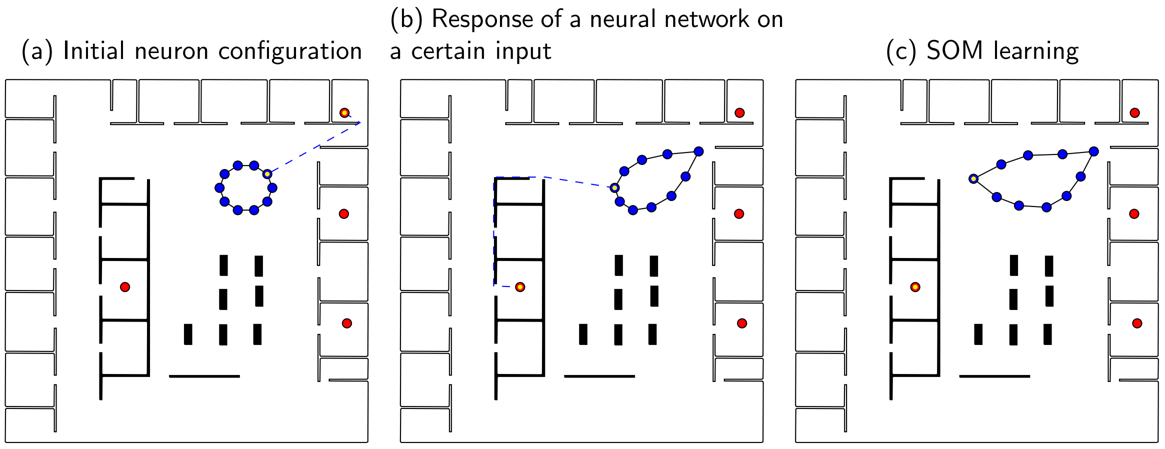
(a) Initial neuron configuration
(b) Response of a neural network on a certain input
(c) SOM learning

Figure 2.2: SOM learning in $\mathcal{S}_m$. The guard that is used as the input and the winning neuron are marked by yellow dots.

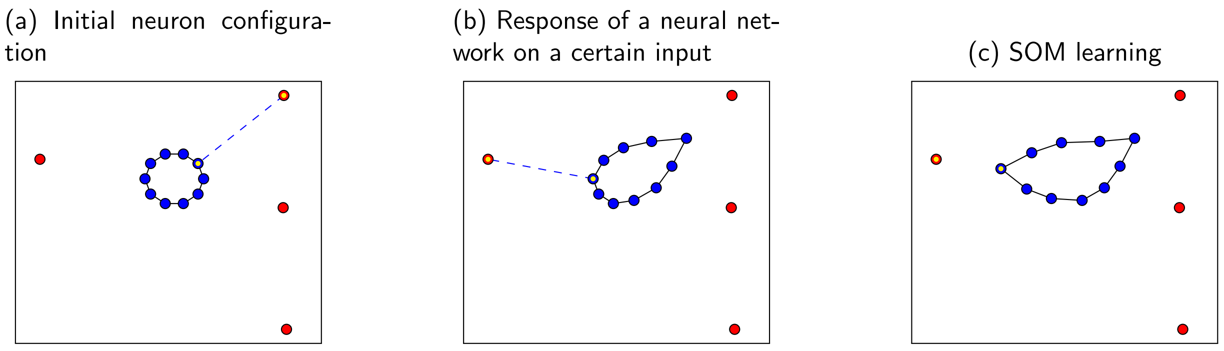
(a) Initial neuron configuration
(b) Response of a neural network on a certain input
(c) SOM learning

update their weights. Other neurons do not change, since SOM uses the Winner-Take-Most model. SOM learns by repeating this process, as shown in Fig. 2.1c.

In order to find the winning neuron for a certain guard, the distance between the guard and the neuron has to be calculated. Distance calculation in a polygonal domain is a computationally intensive task [8][9] (the shortest lines connecting guards with the winning neurons are shown by the blue dashed lines in Fig. 2.1, it is necessary to find these lines and calculate their lengths). On the other hand, it is straightforward to calculate the distances in a domain that has no boundaries or obstacles (as shown in Fig. 2.2). Distances in this domain, $\mathcal{S}_m$, can be calculated much faster according to the used norm. Currently, l_2 and l_∞ are primary norms used in this space. This space is usually multidimensional, dimensionality 6 is normally used. If guards could be mapped into this domain, we might be able to reduce the computation time. This transformation is carried out by the Multidimensional Scaling algorithms. These algorithms produce the coordinates of the guards in a multidimensional space with some norm ($< R^m, l_p >$ space), where $m \in Z$, $m \geq 2$, $p \in Z$ and $p \geq 2$. Distance in this space for $p < \infty$ can be computed as

$$|\mathbf{x}_i - \mathbf{x}_j|_p = \sqrt[p]{\sum_{k=1}^{m} |\mathbf{x}_{ik} - \mathbf{x}_{jk}|^p}, \tag{2.1}$$

for $p = \infty$ it is

$$|\mathbf{x}_i - \mathbf{x}_j|_\infty = \max_k |\mathbf{x}_{ik} - \mathbf{x}_{jk}|. \tag{2.2}$$

The proposed algorithm is shown in Alg. 2. In the first step, the transformation of the map is carried out. The properties of this transformation are discussed later, but briefly, it maps the guards from the polygonal domain into $\mathcal{S}_m$, while trying to preserve the distances between them. In the last step of the algorithm the solution found in $\mathcal{S}_m$ is used to find the tour, so it is not necessary to perform any back transformation into $\mathcal{S}_o$.

Algorithm 1: The proposed algorithm

```
input  : A two-dimensional map with polygonal obstacles and guards
output: A solution of the TSP on the guards
1 Transform the original two-dimensional map with obstacles into $\mathcal{S}_m$;
2 Train SOM on guards in $\mathcal{S}_m$ and find the tour;
```

2.1 Self-Organising Maps

The main element of this method is a ring network that adapts to a set of certain inputs to produce a closed tour around the guards. The adaptation occurs because the forces of two kinds act upon the objects: f_g by the guards and f_n by the neighbouring objects. Objects from that network approach the guards because of f_g acting upon them. On the other hand, f_n reduces the total length of the connections in the network. f_n acts like the forces in an expanded rubber band. Several algorithms are based on that idea: Elastic net [10] and algorithms based on the Self-Organising Map [1] training.

Self-Organising Map [1] (SOM) training is used to produce a closed route that visits each guard exactly once. SOM is a type of a two-layer unsupervised artificial neural network. Structure of SOM is shown in Fig. 2.3. The input layer (red nodes) is used for feeding the coordinates of the guard into the second layer. There are two input neurons in Fig. 2.3, one for each dimension. Self-Organising maps were invented by T. Kohonen in the 1980s. It is traditionally used for clustering and visualisation. N_n neurons lie on a closed tour, each neuron (blue circles in the figure) has two neighbours (a successor and a predecessor) with whom it is connected (connections are shown using black lines). For example, neighbours of the fifth neuron are neurons four and six. Each neuron also has a neighbourhood, which is a set of neurons that are its neighbours, neighbours of neighbours and so on. The size of the neighbourhood is defined by its cardinal distance, which is ring-wise distance (minimal number of connections between two neurons) to the farthest neuron in the neighbourhood. For example, neighbourhood of the fifth neuron and size 2 contains neurons 3, 4, 6, 7.

Each neuron has a weight vector, which can be interpreted as the coordinates of the neuron. SOM uses Winner-Take-Most model, which means that during iteration i, for some input (guard j), we can find the winning neuron k (the closest to the guard) and its weight will approach the guard coordinates more than the weights of any other neuron during that iteration. The neighbours of neuron k will also undergo some change, but to a lesser extent. At the training phase, guards are fed into the SOM repeatedly, so the neurons converge to the guards. The parameters, such as the "force" by which the neurons are pulled, and the size of the neighbourhood, change during the training phase. The algorithm is shown in Alg. 2

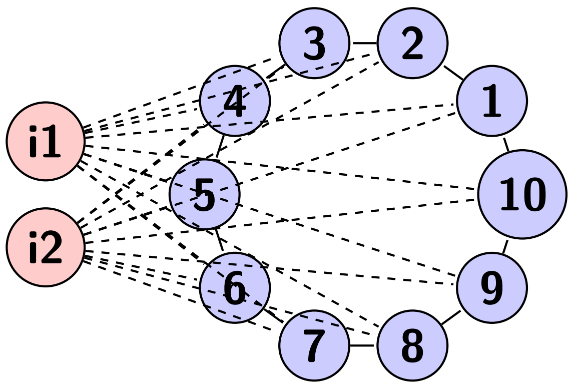

Figure 2.3: SOM example

After the learning phase, it is necessary to infer the tour. Since the neurons form a closed route through the guards, the guards establish a one-to-one relationship with some of the neurons. Therefore, by mapping these neurons to the guards, we may construct the tour by visiting each neuron on the ring and adding the guards that we come across to the tour.

Algorithm 2: SOM training

```
input  : Set of guards in an environment without obstacles
output: A solution of the TSP on the guards
1 Initialise neurons;
2 Pick a guard $g_i$;
3 Find the winning neuron $n_j$;
4 Update weights of the winner and its neighbours so these neurons approach the
  picked guard;
5 If the termination condition is satisfied, construct and return tour;
6 Update parameters and go to step 2.;
```

SOM was first proposed for TSP solving in [2]. The implementation proposed in this article is later referred to as the *Basic SOM*. Other approaches and implementations include a *Co-adaptive neural network* [3] and *Overall-Regional Competitive Self-Organizing Map* [4].

2.1.1 Basic SOM

The algorithm of the basic SOM [2] is shown in Alg. 3

Algorithm 3: Basic SOM and CAN

```
input  : Set of guards in an environment without obstacles
output: A solution of the TSP on the guards
1 Initialise the neural network;
2 Randomise the set of guards;
3 Pick the first guard from the set;
4 Find the winning neuron;
5 Move weights of the winning neuron and its neighbours towards the picked guard;
6 Pick the next guard from the set and go to step 4. If there are no guards left,
  continue to step 7;
7 If the termination condition is satisfied, construct the tour and return it;
8 Otherwise, update the parameters and go to step 2.;
```

In the beginning, the neurons are initialised on a small ring in the centre of the guards distribution. A random permutation of the guards is generated at each iteration. The adaptation process is based on feeding the guards from the permutation into the SOM. For each of the inputs, the winning neuron is selected.

After the winning neuron has been found, its weights and the weights of its neighbours are updated using the following formula:

$$\mathbf{w_j} := \mathbf{w_j} + \mu f(G, d)(\mathbf{X_i} - \mathbf{w_j}) \tag{2.3}$$

where X_i is the coordinates of the chosen guard, $\mathbf{w_j}$ is the weight vector of the neuron, μ is the learning rate, f is the neighbouring function.

$$f(G, d) = \begin{cases} \exp(-d^2/G^2), & \text{if } d < 0.2M \\ 0, & \text{otherwise} \end{cases} \tag{2.4}$$

Here, M is the number of neurons, d is the cardinal distance, G is gain.

The SOM learning is terminated when the maximum error (difference between the coordinates of a guard and the weights of its winning neuron) is smaller than err_{min}.

After each iteration, the gain is updated by the formula

$$G := (1 - \alpha)G. \tag{2.5}$$

2.1.2 Co-adaptive neural network

The co-adaptive neural network [3] (CAN) is another approach to solving the TSP using the SOM. Its main feature is using a so-called cooperation phase. Cooperation means that during the learning process, various inputs cooperate in selecting the winning neuron. Competition and cooperation phases differ in how neurons react when one neuron is the winner for various inputs. In the competition phase, if the neuron was a winner once, only the neighbourhood is moved. If the neuron was chosen more than once, none of the neurons are moved. In the cooperation phase, none of the winning neurons are allowed to move more than once. The neighbours are not allowed to move as well. Both phases are used, competitive in the beginning, the learning method switches to the cooperation phase at some point. The algorithm of the CAN has the same structure as the basic SOM, see Alg. 3

The neurons initialisation in this algorithm is the same as in the basic SOM (initially, the neurons lie on a ring). The winner selection is also similar, but with a change that is supposed to improve the speed: the winning neuron is searched for in the vicinity (not geometrical, but cardinal, ring-wise) of the neuron that was the winner in the previous iteration. Every β iterations the set from which the winning neuron is searched for is expanded to the whole set of neurons.

At the 5th step, The weights of the neurons that have to be moved at iteration t are updated using Eq. 2.6.

$$w_{ik} := w_{ik} + f(g_{jt}, d(j, K))(x_{ik} - w_{ik}) \qquad k = 1, 2 \tag{2.6}$$

$$f(g_{jt}, d(j, K))(x_{ik} - w_{ik}) = \exp(-(d(j, K)/g_{ij})^2)/R \tag{2.7}$$

$$g_{ij} = G_t \left(1 - \sqrt{(x_{i1} - w_{j1})^2 - (x_{i2} - w_{j2})^2}/\sqrt{2}\right). \tag{2.8}$$

The neighbourhood of the winning neuron (the set of neurons that will move) is

$$S = j|d(j, K) < d^*, \quad j = 1, ..., M; j \neq K, \tag{2.9}$$

where

$$d^* = \min(2G_t + 1, D^*, M/2). \tag{2.10}$$

Cooperation phase is used instead of competition when $G_t < G_{\text{cross}}$. In these equations, $\mathbf{w_i}$ is the weights vector, f is the activation function, d is the cardinal distance, K is the winning neuron, G_t is gain at iteration t.

If one of the following conditions is met, the algorithm is terminated.

- the neurons are close enough to the guards, or the maximum error between the guards and their winning neurons is E_{max}
- the weights did not change during the last iteration
- $G_t \leq 0.01$

Gain change is an important part of the adaptation process. In the end of each iteration the gain is updated by Eq. 2.11.

$$G_{t+1} = \begin{cases} (1-\alpha)G_t, & \text{if } G_t \leq G_{\text{cross}}/2 \\ (1-2\alpha)G_t, & \text{otherwise} \end{cases} \tag{2.11}$$

2.1.3 Overall-Regional Competitive Self-Organizing Map

Overall-Regional Competitive Self-Organizing Map [4] (ORC-SOM) is yet another variation of SOM. Its algorithm is shown in Alg. 4. Two new features were introduced in ORC-SOM: overall and regional competition. The winning neurons become less competitive for outlining the tour and more competitive for its refinement due to these new features.

Instead of putting N_n neurons on a ring in the beginning, they are initialised on a rectangle that frames the set of guards. Also, no random permutations of guards are generated, but the input is selected randomly from the set of guards. The SOM adapts for each of these inputs using the update formula in Eq. 2.12.

$$w_j := w_j + Z(n, d_{X,i(X)}, \lambda(n))\eta(n)h_{j,i(X)}(n)[X(n) - w_j], \tag{2.12}$$

where neuron j is from neighbourhood of the winning neuron with size σ.

$$h_{j,i(X)}(n) = \exp(-d^2_{j,i(X)}/2\sigma^2(n)) \tag{2.13}$$

Algorithm 4: ORC-SOM training

```
input  : Set of guards in an environment without obstacles
output: A solution of the TSP on the guards
1 Initialise neurons;
2 Pick a guard at random;
3 Find the winning neuron;
4 Update weights of the winner and its neighbours so these neurons approach the
  picked guard;
5 Update parameters and repeat steps 2 – 4 $it_{max}$ times;
6 Try to construct a tour, if it cannot be constructed, repeat from step 1 with greater
  number of neurons;
7 Return the tour;
```

$$Z(n, d_{X,i(X)}, \lambda(n)) = \exp\left(-\frac{d^2_{X,i(X)}}{2\lambda^2(n)} + 0.5\right) \tag{2.14}$$

$$\lambda(n) = \frac{cd}{4}\left(\frac{2}{1+\exp(-n/2)} - \frac{1}{2}\right) \tag{2.15}$$

Here, $\mathbf{w_j}$ is the weight vector, X is the input guard, $i(X)$ is the winning neuron, d_{ij} is the cardinal distance between two neurons, $d_{X,i(X)}$ is the distance between the guard and the neuron.

Both the learning rate and the neighbourhood size decrease during the iterations by Eq. 2.16 and 2.17. This is done to make the adaptation more "local" in the end of the run.

$$\eta(n) = \eta_0 \exp\left(-\frac{n}{\tau_\eta}\right) \tag{2.16}$$

$$\sigma(n) = \sigma_0 \exp\left(-\frac{n}{\tau_\sigma}\right) \tag{2.17}$$

2.2 Multidimensional scaling

Multidimensional scaling (MDS) is a family of algorithms that map a set of samples into some space based on their similarity. Similarity is usually specified using a positive symmetric distance matrix (also called difference matrix) δ, whose ij-th element contains dissimilarity measure between elements i and j. Since MDS is used to transform the objects from a polygonal domain $\mathcal{S}_o$, the elements of the distance matrix are the distances between the objects in $\mathcal{S}_o$. MDS is traditionally used for visualisation of multidimensional data in two or three-dimensional space (or, mapping multidimensional data into low-dimensional space). In the produced output, similar objects are mapped close to each other forming clusters.

Contrary to the traditional use, the objects are mapped into a *high-dimensional* space in this application. This is done because our goal is to preserve the distances between the objects while abolishing the obstacles and not to visualise their similarity. Distances, which are computed using the visibility graph, are written into the distance matrix. Based on this matrix, **X** (matrix of the coordinates of the objects in $\mathcal{S}_m$) is produced. If the number of objects is N and the desired number of dimensions is m, then **X** is N-by-m matrix and δ is N-by-N matrix.

Algorithm 5: Distance matrix computing

```
input  : Polygonal map and the set of objects in this map
output: Distance matrix
1 Compute the visibility graph $\mathcal{V}$;
2 Compute the distance matrix of $\mathcal{V}$ using the Johnoson's algorithm;
```

The input of the MDS algorithms is a distance matrix, which can be computed by Alg. 5. In the beginning, the visibility graph is calculated. Visibility graph is a graph whose vertices represent objects in a polygonal domain. Vertices that are visible to each other (that can be connected by a line that does not intersect any polygon in the environment) are connected by edges. Distances between these vertices are assigned to the edges between them. Having found the visibility graph, the Johnson's algorithm [11] can be used to calculate the distance matrix.

Distance between the produced coordinates in **X** should be approximately equal to the distance between those two objects in δ according to the used norm l_p,

$$\delta_{ij} \approx ||\mathbf{X}_i - \mathbf{X}_j||_p. \tag{2.18}$$

Quality of the transformation can be measured using the stress function $S(\mathbf{X})$ (Eq. 2.19)

$$S(\mathbf{X}) = \sum_{i<j\leq n} w_{ij}(d_{ij}(X) - \delta_{ij})^2, \tag{2.19}$$

where d is the distance matrix of the objects in $\mathcal{S}_m$. Matrix **X** contains row vectors of the coordinates of the transformed objects,

$$\mathbf{X} = \begin{bmatrix} \mathbf{x}_1 \\ \mathbf{x}_2 \\ \dots \\ \mathbf{x}_N \end{bmatrix}, \tag{2.20}$$

where $\mathbf{x}_1$, $\mathbf{x}_2$, ..., $\mathbf{x}_N$ are the coordinates of the objects in $\mathcal{S}_m$.

Two multidimensional scaling algorithms were implemented: Scaling by Maximizing a Convex Function (SMACOF) [12][13] and Stochastic Force [14]. The reason why SMACOF has been chosen is that it has good performance, it is well-tested, fast and easy to implement. But due to its limitations (which will be covered in the next section), it has been decided to implement an alternative (Stochastic Force).

2.2.1 Scaling by Maximizing a Convex Function

SMACOF is based on stress majorisation. It means that instead of minimising $S(X)$, we can minimise a function $\tau(X, Z)$ that is always greater than or equal to $S(X)$. It can be shown that the following function satisfies that condition:

$$\tau = \eta_\delta^2 + \mathrm{tr}(X^T V X) - 2\mathrm{tr}(X^T B(Z) Z). \tag{2.21}$$

We can find the minimum of τ by setting its derivative to zero:

$$\nabla_X \tau(X, Z) = 0 + 2VX - 2B(Z)Z = 0, \tag{2.22}$$

from which we can find X as

$$X = V^+ B(Z) Z, \tag{2.23}$$

or, if the weights are equal to one,

$$X = N^{-1} B(Z) Z \tag{2.24}$$

SMACOF is an iterative algorithm, and Eq. 2.24 is used as the update formula at each iteration. SMACOF is shown in Alg. 6

Algorithm 6: SMACOF

```
input  : Distance matrix $\delta$
output: Coordinates of the objects in $\mathcal{S}_m$, X
1 Set the iteration number $i = 0$, $Z = X_0$ (random initial configuration);
2 Compute the stress using Eq. 2.19;
3 Increment $i$;
4 Compute the next solution $X_i$ by Eq. 2.24;
5 If the stress change is small, $S_{i-1} - S_i < \varepsilon$, return $X_i$;
6 Go to step 3;
```

Note that in the 5th step, stress difference is computed, and not its absolute value. This is done because stress is always decreasing (in distinction to Stochastic Force, another MDS algorithm). SMACOF was derived using the Cauchy-Schwarz inequality [12], which is true for inner product spaces. Spaces with l_p norm, where $p \neq 2$ are not inner product spaces, therefore they cannot be used by SMACOF. It can be shown that some basic shapes cannot be transformed into desired space without introducing an error. An example of such a shape is a square obstacle, which is covered in Chapter 3.

2.2.2 Stochastic force

Theoretically, SMACOF allows only l_2 norm, so it is impossible to experiment with other norms to find out whether they would yield better results. Because of that, Stochastic Force was implemented. The idea behind this algorithm is that we can simulate spring-like forces between the transformed objects in order to carry out that transformation. The force between a pair of objects pushes them apart if they are closer to each other than in $\mathcal{S}_o$, or towards each other if they are farther than in $\mathcal{S}_o$. The word stochastic comes from the method of computing the forces: they are not calculated for all pairs at each iteration, but rather for two sets: a set of randomly selected objects V_i and a set of pairs of neighbouring objects S_i. This approach has two advantages: it adds jitters to prevent from converging to local optima, while showing good performance for neighbouring objects. V_i is reinitialised at every iteration, while S_i is random at first, but it converges to a set of neighbouring objects in time. It is done by the following rule: while populating V_i, if some candidate to V_i is closer than the farthest object from S_i, add it to S_i instead of V_i. The sizes of these sets are set to V_{max}, S_{max}. The objects movement is simulated using the Euler method.

Euler method is a method for numerical solving of differential equations. Given the system $\frac{\mathrm{d}}{\mathrm{d}t}\mathbf{y}(t) = \mathbf{f}(t, \mathbf{y}(t)$, the solution is approximated by the equation

$$\mathbf{y}_{k+1} = \mathbf{y}_n + h\mathbf{f}(t_n, \mathbf{y}_n) \tag{2.25}$$

here, h is the integration step. Since the spring-like forces are simulated, f and y and be defined as

$$\mathbf{y}_k = \begin{bmatrix} v_k \\ x_k \end{bmatrix} \tag{2.26}$$

$$\mathbf{f}(t, \mathbf{y}_k) = \begin{bmatrix} F_k \\ v_k \end{bmatrix} \tag{2.27}$$

where F_k is the force acting on the object. Therefore, Eq. 2.25 can be rewritten as

$$\begin{bmatrix} v_{k+1} \\ x_{k+1} \end{bmatrix} = \begin{bmatrix} v_k \\ x_k \end{bmatrix} + h \begin{bmatrix} F_k \\ v_k \end{bmatrix}, \tag{2.28}$$

which is used as the update formula at each iteration. Other, more complicated simulation algorithms exist, but it is not necessary to implement them because accurate simulation is not what we are after. For the same reason, h does not have to be too small to yield good results, which is covered later. The procedure is shown in Alg. 7

Algorithm 7: Stochastic Force

```
input  : Distance matrix $\delta$
output: Coordinates of the objects in $\mathcal{S}_m$
1 (Re)initialise $V$, $S$ of all objects;
2 Compute forces acting upon all objects;
3 Make a simulation step;
4 If the termination condition is satisfied, return the coordinates of the objects;
5 If it is not satisfied, go to step 1;
```

At the first step, random objects are added to V (also, S, if it is the first iteration) with a constraint: no repeating objects are allowed in the sets. Reorganise the objects from both sets by adding the closest ones to S and the rest to V.

At the second step, the sum of all forces that act upon object i by objects from V_i and S_i is calculated. The magnitude of the force acting upon object i by object j is proportional to $g_{ij} - \delta_{ij}$ (the difference between the distance in $\mathcal{S}_m$ and in $\mathcal{S}_o$). This force is directed towards the object j. For the purpose of stabilisation, the magnitude of the forces is limited to f_{lim}, so after the sum has been computed, it is necessary to clip some forces.

Next, the simulation step is made. First, compute the velocities using Eq. 2.29.

$$\mathbf{v}_i = \mu(\mathbf{v_i} + \mathbf{f_i}h) \tag{2.29}$$

Here, μ is the friction constant, whose purpose is stabilisation of the system. After the velocities have been updated, compute the new coordinates using the expression

$$\mathbf{x}_i = \mathbf{x_i} + \mathbf{v_i}h \tag{2.30}$$

The advantage of this algorithm over SMACOF is that it allows using norms other than the Euclidean.

Chapter 3

Implementation

Algorithms described in the previous sections were implemented. The program was written in C++ programming language with external C++ libraries: *VTK*, *Boost*, *Eigen*, *VisiLibity*. *Triangle* library written in pure C was also used.

VTK (Visualization Toolkit, `http://www.vtk.org/`) is an open-source, cross-platform C++ library (interfaces for Tcl/Tk, Java and Python are also available) developed by Kitware. VTK is used for visualisation, image processing and computer graphics. Although VTK is very feature rich, it was used mainly for visualisation of the algorithms. The recommended version of this library is 6.0+, but it is mostly compatible with version 5.8. The implementation can be compiled without *VTK*, since it is used only for visualisation.

Boost (`http://www.boost.org/`) is a set of cross-platform open-source C++ libraries. The range of its applications is wide. It is used for graph algorithms, linear algebra operations, math algorithms, multithreading and other purposes. It contains over 80 libraries. In this implementation, it is used for reading of the command-line switches (in Boost.Program_options) and for its graph algorithms (Boost.Graph).

Eigen C++ library (`http://eigen.tuxfamily.org/`) is used for matrix calculations. It is an open-source template library used for algorithms related to linear algebra. It is widely used in scientific projects and by corporations for machine learning, robotics, numerical computation and other applications.

VisiLibity (`http://www.visilibity.org/`) enables us to compute the visibility graph of a polygonal map. It is a free open-source C++ library for visibility algorithms. It is used for planning, navigation, manufacturing and other areas. It is aimed to enable programmers to perform simple visibility calculations in the polygonal domain.

Triangle (`https://www.cs.cmu.edu/~quake/triangle.html`) is used for calculation of the Delaunay triangulation of a polygonal map. It is an open-source C library developed at Carnegie Mellon University. It can be used both as a library and an executable for creating the Delaunay triangulations, the constrained Delaunay triangualations, Voronoi diagrams and triangular meshes. It supports various parameters of the available algorithms (e.g. forcing edges for Delaunay triangulation, setting the smallest allowed angle of triangles and others).

CMake (`http://www.cmake.org/`) is used as a build manager, but it is possible to build the project without it.

The input (environment and guards) format is based on the map (.txt) format used in the Intelligent and Mobile Robotics Group (`http://imr.ciirc.cvut.cz/planning/maps.xml`). The rules are more strict though. The map file contains vertices that describe the map. The file is divided into sections. A section represents a polygon (first section contains the description of the map borders and the following sections describe borders). Each section starts with a line `[borders]`. Each of the following lines in the section contain two real numbers divided by a space (the coordinates of the vertex). The sections finish in an empty line. No repeating vertices or obstacles are allowed.

The guards file starts with a line `[guards]` that follows by N_n lines that contain the coordinates of the guards. Each of these lines contains two real numbers (as in the map file).

Both files have two empty lines in the bottom. The guards must lie within the map boundaries. The polygons from the map file cannot overlay. The vertices of the map boundaries and the obstacles must be listed counterclockwise.

3.1 Self-Organising maps

The original algorithms were designed for the two-dimensional Euclidean space $< R^2, l_2 >$, but other spaces were also used in this implementation, so it was necessary to make some changes to the algorithms. In the beginning of the network learning, the neurons have to be initialised. Depending on the used algorithm, they can be initialised either on a small ring, or on a frame around the guards. This initialisation is unambiguous in a two-dimensional space, but in $\mathcal{S}_m$ different initial weights are possible. The easiest one is to ignore higher dimensions (set the corresponding weights to zero) and initialise the neurons as though the neurons are in the two-dimensional space. Because of the increased number of dimensions, the structure of SOM changes as well: instead of 2 input neurons in Fig. 2.3, it is necessary to use m neurons in the input layer, since SOM is used in $\mathcal{S}_m$ with m dimensions.

3.2 Multidimensional scaling

Input of the MDS algorithms is a distance matrix δ, whose elements contain distances between the transformed objects ($\delta_{ij} = d(i,j)$). In order to produce that matrix, the following libraries and algorithms were used:

- VisiLibity, a library for 2D visibility algorithms. Algorithm for visibility graph computation from this library has time complexity $O(n^3)$,

- Johnoson's algorithm for distance matrix computing from Boost library.

There are two ways of transforming the guards from $\mathcal{S}_o$ into $\mathcal{S}_m$: the first method is environment-based (indirect method), which means that the coordinates of the guards in $\mathcal{S}_m$ are not computed directly, but the estimate of their location is based on the existing transformation of the environment, as shown in Alg. 8. In the alternative approach (Alg. 9), the guards are transformed directly (guards-based method).

Algorithm 8: Guards transformation, environment-based approach

```
input  : A polygonal map, a set of guards
output: Mapping of the guards into $\mathcal{S}_m$
1 Compute the distance matrix of the vertices of the polygons of the map by Alg.5;
2 Transform the distance matrix into $\mathcal{S}_m$ using MDS;
3 Create Delaunay triangulation of $\mathcal{S}_o$ map, forcing edges of the obstacles to be edges
  of triangles;
4 Approximate the coordinates of the guards in $\mathcal{S}_m$;
```

Algorithm 9: Guards transformation, guards-based approach

```
input  : A polygonal map, a set of guards
output: Mapping of the guards into $\mathcal{S}_m$
1 Compute the difference matrix of the guards by Alg.5;
2 Transform the difference matrix into $\mathcal{S}_m$ using one of the MDS methods;
```

Both methods have advantages and disadvantages. The direct method allows us to transform the map into $\mathcal{S}_m$ once, and use it for various sets of guards, saving some time. It is faster to approximate the coordinates of the guards in $\mathcal{S}_m$ than to actually transform them using MDS for every new set of guards on the same map. On the other hand, the second approach might produce better results in some cases, since the coordinates are not approximated but computed directly. It is worth mentioning that the results will not necessarily be improved by using the second method. For example, if the used map is *jari* from Fig. 2.1, and there is maximum one guard per room, the error introduced by approximation of the coordinates of the guards is small relatively to the distances between the guards, therefore, the first approach should be used.

If the environment-based approach is used, the coordinates of the guards have to be approximated. First, the triangulation of the map is created and for each guard i a triangle t in which it lies is found.

$$\begin{bmatrix} x_i \\ y_i \end{bmatrix} = \begin{bmatrix} aA_x + bB_x + cC_x \\ aA_y + bB_y + cC_y \end{bmatrix}, \tag{3.1}$$

$$a + b + c = 1, \tag{3.2}$$

where $(x_i, y_i)^T$ is the coordinates vector of the guard i, $(A_x, A_y)^T, (B_x, B_y)^T, (C_x, C_y)^T$ are the coordinates of the vertices of the triangle t and a, b, c are the weights that have to be found. Eqs. 3.1 and 3.2 can be rewritten as

$$\begin{bmatrix} x_i \\ y_i \\ 1 \end{bmatrix} = \begin{bmatrix} A_x & B_x & C_x \\ A_y & B_y & C_y \\ 1 & 1 & 1 \end{bmatrix} \begin{bmatrix} a \\ b \\ c \end{bmatrix}, \tag{3.3}$$

and the weights can be computed as

$$\begin{bmatrix} a \\ b \\ c \end{bmatrix} = \begin{bmatrix} A_x & B_x & C_x \\ A_y & B_y & C_y \\ 1 & 1 & 1 \end{bmatrix}^{-1} \begin{bmatrix} x_i \\ y_i \\ 1 \end{bmatrix}. \tag{3.4}$$

Coordinates in $\mathcal{S}_m$ can be computed as

$$\mathbf{x}_{im} = a\mathbf{A}_m + b\mathbf{B}_m + c\mathbf{C}_m \tag{3.5}$$

3.2.1 SMACOF

It was found that the proposed termination criterion is not robust. The authors suggested to halt the algorithm when the stress difference is small, $S_{i-1} - S_i < \varepsilon$. Since the value of stress can vary in different environments, setting ε to some predefined value may be inadequate. It is also difficult to guess the appropriate value of ε for a chosen map. Because of that, the termination method was changed to $\frac{S_{i-1}-S_i}{S_i} < \varepsilon$.

Limitations

As mentioned earlier, some obstacles cannot be transformed into $\mathcal{S}_m$ with l_2 norm. An example of such an object is a square obstacle. Distance matrix of the vertices of a square with sides of unity length is

$$D = \begin{bmatrix} 0 & 1 & 2 & 1 \\ 1 & 0 & 1 & 2 \\ 2 & 1 & 0 & 1 \\ 1 & 2 & 1 & 0 \end{bmatrix} \tag{3.6}$$

The best result can be achieved by setting the number of dimensions to three. Setting it to a greater number will not improve the transformation since four vertices will always lie in a three-dimensional subspace. In order to carry out that transformation, we can start by putting the vertices on a unit square:

$$\mathbf{X} = \begin{bmatrix} \mathbf{x}_1 \\ \mathbf{x}_2 \\ \mathbf{x}_3 \\ \mathbf{x}_4 \end{bmatrix} = \begin{bmatrix} 0 & 0 & 0 \\ 0 & 1 & 0 \\ 1 & 1 & 0 \\ 1 & 0 & 0 \end{bmatrix} \tag{3.7}$$

In this configuration, the adjacent vertices have the requested distance $d_a = 1$, but the distance between the opposite vertices is $d_o = \sqrt{2}$. Since any deviation from this initial configuration will lead either to increasing d_a, or decreasing d_o, it is impossible to find a proper transformation.

This leads us to experimenting with other metrics. Theoretically, SMACOF works only in l_2. Despite that, SMACOF was tested with other metrics (l_3, l_8, l_∞), but it did not improve its performance. It is theoretically possible to transform the square into $< R^2, l_\infty >$ space, as shown in Fig. 3.1b. Therefore, another algorithm (which is less dependent on the metric) is required. Stochastic Force was chosen due to that.

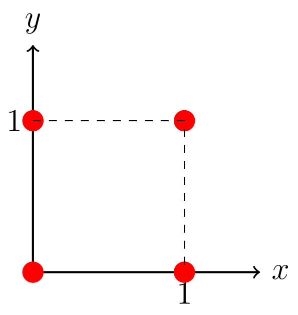

(a) Transformation in l_2

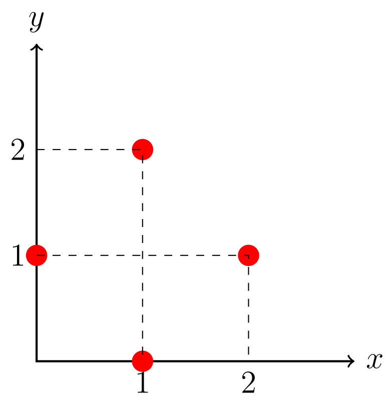

(b) Transformation into a space with the metric l_∞ has zero error

Figure 3.1: Different transformations of a square obstacle into $\mathcal{S}_m$

3.2.2 Stochastic force

In the proposed algorithm, the Euler method is used for simulation. It raises the problem of choosing the suitable integration step size h. The solution is to start with rather big h (e.g. 30, while normally it would be 0.3) and reduce h each time when the stress increases (as shown in the first step of Alg. 10). The termination method was another problem that was confronted during the testing. It was found by the experiment that the stress can increase for several iterations in a row, and then decrease significantly afterwards. Because of that, it is not apt to terminate the algorithm as soon as the stress starts to increase. That is why the termination condition was set to

$$\left| \frac{S_{i-1} - S_i}{S_i} \right| < \varepsilon \qquad (3.8)$$

The employed method of the termination is shown in Alg. 10.

This approach has several advantages. In the beginning, objects move to their appropriate positions "globally" faster than they would if the h was smaller. But each time when the stress increases, h decreases allowing more precise positioning locally. Another big advantage of this

Algorithm 10: Stochastic force termination

```
1 If the stress has increased in the last integration step, reduce $h$ by $\alpha$ %;
2 If the absolute value of the ratio of the stress difference and stress is smaller than
  epsilon (Eq. 3.8) for $k_{term}$ times in a row, terminate the algorithm;
```

method is that the constants used in that part of the algorithm may be used in problems of different scales. This also allows us to use Eq. 3.8 since h is constantly reducing, and the displacement of the coordinates made in each iteration is reducing as well.

Another extension was made due to the usage of the metrics other than Euclidean. Normally, the force vector acting on object i by object j is directed towards object j. It is quite natural, because this is how the spring forces would actually act upon the objects (in the Euclidean space). But for the metric l_∞, a different approach can be used. Distance between two objects is computed by Eq. 3.9.

$$|\mathbf{X}_i - \mathbf{X}_j|_\infty = \max_k |\mathbf{X}_{ik} - \mathbf{X}_{jk}| \tag{3.9}$$

Therefore, there is a dimension that "defines" that distance, $K = \mathrm{argmax}_k |\mathbf{X}_{ik} - \mathbf{X}_{jk}|$, or $|\mathbf{X}_i - \mathbf{X}_j|_\infty = |\mathbf{X}_{iK} - \mathbf{X}_{jK}|$. K is important because in many cases changing the coordinates in the other dimensions will not influence the distance. Specifically, we can freely move object i towards object j in the dimensions other than K, and the distance between them will not decrease. Because of that, two methods of force computing were implemented, and the appropriate method is used depending on what metric is used.

If the metric is not l_∞, then the force that acts upon the object i is directed towards the object j. If the used metric is l_{inf}, then the force vector has the form

$$f_{ik} = \begin{cases} f, & \text{if } k = K = \mathrm{argmax}_k(|x_{ik} - x_{jk}|) \\ 0, & \text{otherwise} \end{cases} \tag{3.10}$$

Either way, the magnitude of the force is proportional to $g_{ij} - \delta_{ij}$ (the difference between the distance in $\mathcal{S}_m$ and in $\mathcal{S}_o$).

Chapter 4

Experiments

The algorithms described in the previous chapters were tested. Since a great number of experiments was required, a lot of processing power was necessary. This was made possible thanks to the National Grid Infrastructure MetaCentrum, which provided a cluster for parallel computation of the experiments.

4.1 Evaluation of the multidimensional scaling algorithms

First, it is necessary to analyse the MDS algorithms. As already mentioned, two MDS algorithms were implemented: Stochastic Force and SMACOF. Different space dimensions and norms were used: Stochastic Force was tested with dimensions R^2, R^3, R^6, R^{10} and norms l_2, l_3, l_8, l_∞. SMACOF was tested with dimensions R^2, R^3, R^6, R^{10} and l_2 norm.

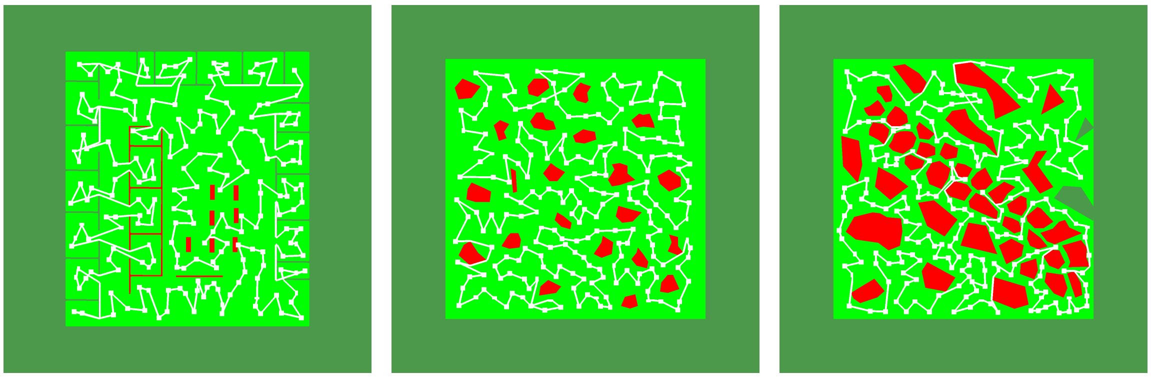
(a) *jari* (b) *potholes* (c) *var_density*

Figure 4.1: Maps used for testing

Three maps were used in the experiments: *jari*, *potholes* ans *var_density*. They are shown in Fig. 4.1. 200 guards were initialised in each of the maps. Paths shown in these figures are examples of the solutions found using the developed procedure. They were found by ORCSOM and guards-based Stochastic Force.

There are two ways of using the MDS for the guards transformation: the environment-based method and the guards-based method. In the former, the vertices of the environment are transformed into $\mathcal{S}_m$, and estimation of the coordinates of the guards is based on this transformation and their relative positions to the vertices of the map in $\mathcal{S}_o$. In the guards-based method, the guards are transformed directly. Summary of the experiments is shown in Table 4.1.

Algorithm	Transformation based on	Transformation of	Tables
Stochastic Force	Environment	Environment	4.3 . . . 4.5
		Guards	<u>4.6 . . . 4.8</u>
	Guards	Environment	–
		Guards	4.9 . . . 4.11
SMACOF	Environment	Environment	4.12 . . . 4.14
		Guards	<u>4.15 . . . 4.17</u>
	Guards	Environment	–
		Guards	4.18 . . . 4.20

Table 4.1: Tables of experiments of the MDS algorithms

The presented results were obtained by repetitive launching (30 times each) of the MDS with the same parameters. Each of the runs was evaluated by comparing the obtained distance matrix d to the original distance matrix δ. The relative error (Eq. 4.1) mean, the maximum error and the standard deviation of the error are calculated. These values correspond to the columns *ave1*, *max1*, *var1*. The mean, standard deviation and the maximum value of the absolute error (Eq. 4.2) relative to the length of the diagonal D of the map were computed as well. These values correspond to the columns *ave2*, *max2*, *var2*. Relative errorE_1, absolute error E_2 and stress S are used for comparison of the various approaches.

$$E_1 = |d_{ij} - \delta_{ij}|/|\delta_{ij}| \tag{4.1}$$

$$E_2 = |d_{ij} - \delta_{ij}|/D \tag{4.2}$$

The results of the tables whose references are underlined (environment-based transformation of the guards) are the most important for us. They are more important than the others because they are the fastest of all. Results of Tables 4.9 . . . 4.11 and 4.18 . . . 4.20 (guards-based transformation of the guards) are shown for comparison with the environment-based method. Tables 4.3 . . . 4.5 and 4.12 . . . 4.14 (transformation of the environment) show how the guards approximation degrades the quality of the environment-based transformation. For example, consider Tables 4.3 and 4.6. Transformation of the environment is shown in the former and the approximation of the guards based on that transformation is in the latter. The absolute error of the guards is larger than the absolute error of the environment. The relative error is not suitable for that comparison because the objects that are close to each other are prone to having larger relative error, and the vertices of the map can be often quite close.

From the obtained values we can make some observations and evaluate the quality of the transformations. First of all, the stress decreases when the larger number of dimensions is used. The question is when this effect becomes small. Usually, the quality of the guards transformation (measured by the error) does not improve significantly by using the number of dimensions larger than 6. In one case using R^{10} reduced the stress almost by half comparing to R^6), so it was decided to keep experimenting with the number of dimensions $m = 10$. Different maps require different m. The greater number of dimensions is necessary for the *jari*-type maps that have complex non-convex obstacles (for example, maps with rooms). If the obstacles are mostly convex, the necessity of using a greater number of dimensions decreases. For example, using R^6 instead of R^3 reduces stress by 5% in *potholes*, and by 42% in *jari* (Tables 4.4, 4.3)

It is difficult to choose the most suitable norm, because it varies in different maps. Using l_∞ seems to produce better transformations in *jari* (Tables 4.3, 4.6, 4.9), but it is worse in *potholes* (Tables 4.4, 4.7, 4.10). The performance of l_3 and l_8 was always worse than the performance of the other tested norms. Quality improvement of l_∞ comparing to l_3 and l_8 is caused by using modified forces in the Stochastic Force algorithm for l_∞. It is also important to notice that if the environment-based transformation is used, some quality loss is inevitable. Since the used method of the guards estimation was developed for l_2, the quality loss is larger when l_∞ is used.

The most significant difference between the direct and the indirect method can be observed in the *potholes* map, where the stress is about 10 times greater in the environment-based approach, which is observed in both Stochastic Force and SMACOF. (Tables 4.7, 4.10 and 4.7, 4.10) While in the other maps the difference is not so noticeable, it is difficult to guess how this error induced by guards approximation will affect the tour length of the obtained solution without actually testing both methods.

Similarly to Stochastic Force, the recommended choice of the number of dimensions for SMACOF is around 6. An interesting observation is that SMACOF performs much worse then Stochastic Force in R^2. This is caused by inability of SMACOF to break out of the local optima.

Mostly, the quality of the transformation by SMACOF and Stochastic Force is similar, with the exception of the *jari* map, where l_∞ is more suitable, and therefore, cannot be used in SMACOF. In the used implementation, SMACOF is much faster than Stochastic Force. Unlike SMACOF, Stochastic Force has many parameters that can be tuned (V_{max}, S_{max}, α and others), so its quality can be improved for various maps.

Comparison of the stress progression is shown in Fig. 4.2. The test was performed in the *jari* map with $< R^{10}, l_2 >$. SMACOF produces a quality solution much faster than Stochastic Force. Stochastic Force required appropriately 15000 iterations, but it could have been terminated earlier (after the first 5000 iterations) without dramatic quality decline, so the time consumed by Stochastic Force could have been reduced by three times.

The experiments have been performed on a cluster whose nodes have different characteristics. It is therefore impractical to compare the methods based on the time consumed on the cluster.

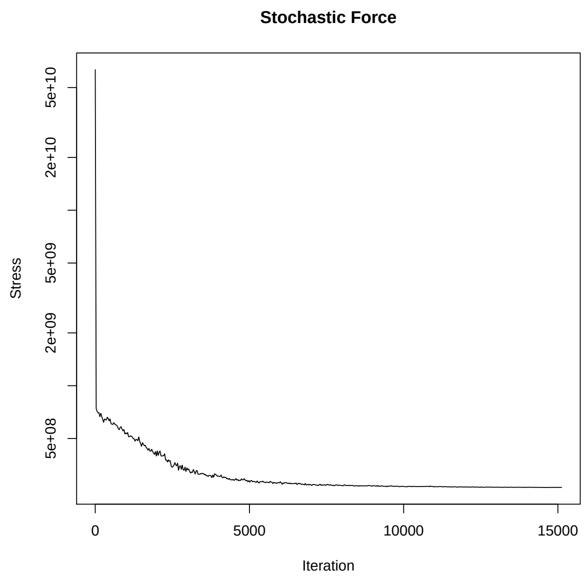

(a) *Stochastic Force*

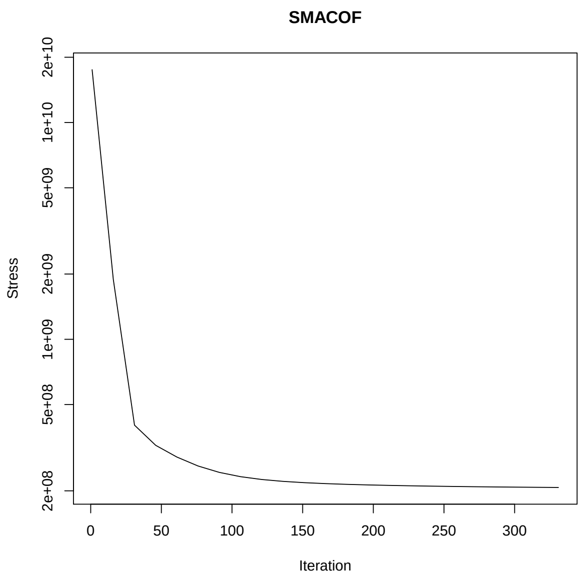

(b) *SMACOF*

Figure 4.2: Stress progression

In addition to that, the performance is dependent on the implementation, so it is difficult to analyse time characteristics of the developed methods. Only approximate values are known, and they can be improved, but since this is not the goal of the thesis, it has been left for the future development.

Testing on the single map *jari* with 200 guards, on $< R^3, l_2 >$ space, the time intervals consumed by the various parts of the algorithm are shown in Table 4.2. Time needed for data preparation is specified in the last column. It includes calculation of the visibility graphs, guards estimation, input files reading and other necessities. The CPU used for this experiment is Intel(R) Core(TM) i5-4200U CPU @ 1.60GHz. The implementations of ORCSOM and SMACOF are the fastest among their analogues.

4.2 Evaluation of the self-organising map algorithms

Analysis has shown that the most promising parameters of the output space of the MDS algorithms are: l_2 and l_∞ and R^6 to R^{10}. Therefore, MDS with these parameters were used for the SOM testing. For each of the MDS outputs obtained in the previously discussed tests, SOM, ORCSOM and CAN algorithms were used to find the tour.

As shown in Tables 4.21 ... 4.24, there is some difference in the quality of solution between the various methods, but it is relatively small. For example, there is 13% difference between the shortest (CAN, R^{10}, l_2, environment-based Stochastic Force) and the longest (SOM, R^6,

l_2, guards-based SMACOF) tour length for *jari*. For Stochastic Force, l_∞ does not seem to decrease the tour length, otherwise, the results produced when using this norm are generally worse than the results of the traditional Euclidean norm. Moreover, two unusually lengthy tours were found using the guards-based Stochastic Force in R^{10}, l_∞ in *potholes* and *var_density*. This error appears because the SOM algorithms were developed for the two-dimensional Euclidean space, so maybe some changes are necessary to improve their behaviour in other spaces, but in the current implementation l_2 is the better choice.

SOM, CAN and ORCSOM produce results of the similar quality in *potholes*, *var_density*, but in *jari* the results produced by the basic SOM are worse. Therefore, CAN and ORCSOM seem to be more robust. R^{10} is slightly better than R^6 in most instances, but the difference is not significant.

Guards-based approach was expected to improve the results, but it is not the case. Even when it does produce the shorter tour, the time that was consumed by the MDS does not pay off in the quality improvement. And finally, the choice of the MDS algorithm does not influence the quality, therefore, the less time-consuming (SMACOF) should be chosen.

Table 4.2: Approximate time consumed by the various modules

	Stochastic Force	SMACOF	SOM	CAN	ORCSOM	The rest
time (s)	35	1	3	6	1	3

m	p	AVG1	MAX1	VAR1	AVG2	MAX2	VAR2	S
		$\times 10^{-2}$	$\times 10^{-1}$	$\times 10^{-3}$	$\times 10^{-2}$	$\times 10^{-1}$	$\times 10^{-3}$	$\times 10^{6}$
2	2	9.47	39.61	13.53	3.81	2.87	1.27	881.41
	3	10.03	33.76	13.62	4.14	2.90	1.41	1013.67
	8	11.93	28.99	14.07	5.24	3.22	1.81	1476.29
	∞	12.67	23.96	18.59	5.53	3.45	2.46	1862.22
3	2	7.12	30.22	6.63	2.93	2.04	0.65	486.43
	3	7.71	30.79	7.12	3.26	2.11	0.77	593.77
	8	9.83	40.39	8.46	4.44	2.33	1.23	1042.16
	∞	7.53	22.07	7.95	3.25	2.66	0.99	661.44
6	2	5.63	21.23	3.99	2.28	1.37	0.36	283.18
	3	6.01	20.37	4.11	2.54	1.43	0.44	352.39
	8	8.50	26.28	5.50	4.04	1.80	1.04	873.14
	∞	2.53	10.12	1.27	1.11	1.67	0.18	99.92
10	2	5.49	21.41	3.81	2.22	1.20	0.32	263.39
	3	5.82	21.50	3.86	2.45	1.25	0.39	322.48
	8	8.33	22.65	5.22	3.97	1.75	1.03	846.69
	∞	1.35	4.56	0.33	0.65	1.04	0.08	40.04

Table 4.3: Transformation of environment by Stochastic Force (environment-based) on the map *jari*

m	p	AVG1 $\times 10^{-2}$	MAX1 $\times 10^{-1}$	VAR1 $\times 10^{-3}$	AVG2 $\times 10^{-2}$	MAX2 $\times 10^{-1}$	VAR2 $\times 10^{-3}$	S $\times 10^{6}$
2	2	3.05	5.48	2.65	0.86	2.55	0.32	35.11
	3	4.72	5.67	2.71	1.42	2.50	0.33	48.42
	8	8.01	8.12	4.30	2.53	2.57	0.55	107.73
	∞	8.88	7.01	7.01	2.73	2.35	0.74	136.68
3	2	2.47	5.23	1.34	0.61	0.93	0.06	8.66
	3	3.55	6.57	1.61	0.95	0.92	0.08	15.08
	8	6.26	10.22	3.29	1.79	1.15	0.24	50.32
	∞	4.32	5.88	1.85	1.31	1.60	0.19	32.80
6	2	2.40	4.89	1.48	0.58	0.94	0.06	8.24
	3	3.14	6.38	1.68	0.81	0.93	0.07	12.57
	8	4.87	8.38	2.81	1.33	1.01	0.15	30.16
	∞	2.01	3.49	0.41	0.61	0.90	0.04	6.95
10	2	2.40	4.89	1.49	0.58	0.94	0.06	8.23
	3	3.06	5.91	1.59	0.78	0.85	0.06	11.21
	8	4.71	7.95	2.68	1.29	1.06	0.15	28.68
	∞	1.76	3.07	0.33	0.54	0.83	0.03	5.78

Table 4.4: Transformation of environment by Stochastic Force (environment-based) on the map *potholes*

m	p	AVG1 $\times 10^{-2}$	MAX1 $\times 10^{-1}$	VAR1 $\times 10^{-3}$	AVG2 $\times 10^{-2}$	MAX2 $\times 10^{-1}$	VAR2 $\times 10^{-3}$	S $\times 10^{6}$
2	2	3.13	5.86	1.49	0.76	1.44	0.06	37.01
	3	4.64	8.22	1.96	1.28	1.48	0.13	93.26
	8	7.30	11.27	3.76	2.13	1.61	0.37	261.79
	∞	7.44	8.66	4.92	2.11	1.72	0.42	274.58
3	2	2.89	5.89	1.20	0.69	0.98	0.04	28.68
	3	3.65	6.10	1.49	0.93	0.97	0.07	50.17
	8	5.85	8.25	3.01	1.62	1.50	0.24	161.55
	∞	3.81	5.25	1.58	1.08	1.26	0.12	74.22
6	2	2.80	5.81	1.12	0.65	0.75	0.04	24.96
	3	3.40	6.12	1.29	0.86	0.79	0.06	42.32
	8	5.19	7.94	2.36	1.42	1.32	0.18	124.39
	∞	2.10	4.09	0.57	0.59	0.87	0.04	22.98
10	2	2.80	5.82	1.11	0.65	0.73	0.04	24.76
	3	3.32	5.89	1.26	0.83	0.76	0.05	39.18
	8	5.22	7.43	2.32	1.43	1.28	0.18	124.23
	∞	2.00	3.49	0.51	0.57	0.82	0.04	21.89

Table 4.5: Transformation of environment by Stochastic Force (environment-based) on the map *var_density*

m	p	AVG1 $\times 10^{-2}$	MAX1 $\times 10^{-1}$	VAR1 $\times 10^{-3}$	AVG2 $\times 10^{-2}$	MAX2 $\times 10^{-1}$	VAR2 $\times 10^{-3}$	S $\times 10^{6}$
2	2	7.95	9.61	7.39	3.02	2.01	0.70	269.24
	3	8.73	8.98	7.99	3.37	2.04	0.85	333.52
	8	11.44	9.17	9.70	4.63	2.53	1.38	589.80
	∞	12.87	11.16	15.79	5.20	2.84	2.20	860.20
3	2	6.72	6.56	3.72	2.60	1.86	0.44	187.06
	3	7.33	7.16	4.40	2.87	1.87	0.56	232.60
	8	10.13	8.30	6.65	4.13	2.09	1.10	471.30
	∞	8.27	9.83	6.84	3.24	2.21	0.84	318.21
6	2	6.30	6.39	3.11	2.37	1.79	0.37	155.15
	3	6.82	6.44	3.43	2.66	1.78	0.48	198.75
	8	9.62	7.35	5.43	3.99	1.92	1.02	439.17
	∞	4.97	9.49	3.55	1.89	1.87	0.39	124.76
10	2	6.25	6.09	3.09	2.34	1.78	0.36	152.45
	3	6.68	6.31	3.32	2.58	1.77	0.44	185.56
	8	9.63	7.16	5.42	4.02	1.95	1.05	446.68
	∞	4.38	10.41	3.43	1.64	1.83	0.31	97.08

Table 4.6: Transformation of guards by Stochastic Force (environment-based) on the map *jari*

m	p	AVG1 $\times 10^{-2}$	MAX1 $\times 10^{-1}$	VAR1 $\times 10^{-3}$	AVG2 $\times 10^{-2}$	MAX2 $\times 10^{-1}$	VAR2 $\times 10^{-3}$	S $\times 10^{6}$
2	2	4.76	9.80	4.44	1.35	1.10	0.27	75.33
	3	6.42	10.41	4.76	1.87	1.15	0.33	112.76
	8	10.35	12.80	7.27	3.15	1.70	0.69	282.41
	∞	12.22	20.56	16.46	3.67	2.06	1.30	467.16
3	2	5.11	46.32	20.46	1.11	1.91	0.33	76.50
	3	6.53	47.17	24.05	1.54	2.18	0.40	106.68
	8	10.57	47.10	30.34	2.76	2.60	0.88	275.67
	∞	7.96	43.12	19.48	2.14	2.17	0.52	164.60
6	2	5.05	45.62	20.27	1.09	1.88	0.34	75.94
	3	6.20	46.12	20.93	1.47	1.96	0.38	100.33
	8	8.18	50.52	24.23	2.07	2.19	0.52	160.21
	∞	6.87	48.25	29.77	1.60	2.43	0.51	128.17
10	2	5.05	45.59	20.26	1.09	1.88	0.33	75.84
	3	6.21	47.05	21.99	1.46	2.02	0.38	99.62
	8	8.05	45.29	21.75	2.05	2.03	0.52	157.61
	∞	6.90	49.78	30.99	1.60	2.44	0.52	129.54

Table 4.7: Transformation of guards by Stochastic Force (environment-based) on the map *potholes*

m	p	AVG1 $\times 10^{-2}$	MAX1 $\times 10^{-1}$	VAR1 $\times 10^{-3}$	AVG2 $\times 10^{-2}$	MAX2 $\times 10^{-1}$	VAR2 $\times 10^{-3}$	S $\times 10^{6}$
2	2	3.40	5.11	1.14	1.05	1.28	0.09	33.14
	3	5.48	4.91	1.90	1.82	1.23	0.25	97.16
	8	9.37	5.83	4.25	3.19	1.31	0.66	282.17
	∞	10.03	8.55	5.46	3.32	1.61	0.70	302.67
3	2	3.11	5.30	1.03	0.90	1.06	0.06	23.64
	3	4.42	6.25	1.68	1.34	0.99	0.13	51.31
	8	8.19	7.90	4.74	2.62	1.47	0.48	196.96
	∞	5.12	6.33	2.16	1.67	1.44	0.23	85.28
6	2	3.01	4.78	0.99	0.85	0.95	0.05	20.96
	3	4.18	5.39	1.47	1.25	1.00	0.11	45.22
	8	7.20	9.67	4.00	2.26	1.38	0.37	150.63
	∞	3.66	18.34	2.30	1.12	1.15	0.11	39.28
10	2	3.01	4.80	0.99	0.85	0.97	0.05	20.94
	3	4.02	5.28	1.40	1.20	1.01	0.10	40.96
	8	7.26	7.95	3.92	2.28	1.38	0.37	150.87
	∞	3.61	17.08	2.30	1.10	1.09	0.11	38.21

Table 4.8: Transformation of guards by Stochastic Force (environment-based) on the map *var_density*

m	p	AVG1 $\times 10^{-2}$	MAX1 $\times 10^{-1}$	VAR1 $\times 10^{-3}$	AVG2 $\times 10^{-2}$	MAX2 $\times 10^{-1}$	VAR2 $\times 10^{-3}$	S $\times 10^{6}$
2	2	6.55	7.60	6.09	2.48	1.79	0.56	197.00
	3	7.27	7.75	6.57	2.83	2.03	0.70	251.62
	8	9.89	7.84	7.60	4.09	2.48	1.15	472.01
	∞	9.98	8.79	8.29	4.16	2.98	1.41	525.61
3	2	5.29	5.64	2.93	2.11	1.52	0.40	141.36
	3	5.94	5.79	3.29	2.40	1.55	0.49	178.29
	8	8.07	7.51	4.74	3.31	2.02	0.84	325.46
	∞	5.90	8.85	3.99	2.40	2.15	0.57	191.94
6	2	4.73	4.71	1.91	1.90	1.16	0.33	115.35
	3	5.21	5.01	2.20	2.15	1.27	0.41	145.58
	8	7.24	6.49	3.65	3.08	1.70	0.78	290.73
	∞	2.25	4.04	0.63	0.97	1.19	0.15	40.59
10	2	4.69	4.79	1.86	1.89	1.15	0.32	113.41
	3	5.19	4.82	2.10	2.13	1.27	0.39	142.01
	8	7.26	6.02	3.70	3.13	1.69	0.84	305.42
	∞	1.58	2.36	0.30	0.70	1.00	0.09	23.45

Table 4.9: Transformation of guards by Stochastic Force (guards-based) on the map *jari*

m	p	AVG1 $\times 10^{-2}$	MAX1 $\times 10^{-1}$	VAR1 $\times 10^{-3}$	AVG2 $\times 10^{-2}$	MAX2 $\times 10^{-1}$	VAR2 $\times 10^{-3}$	S $\times 10^{6}$
2	2	0.80	3.39	0.17	0.22	0.53	0.01	1.89
	3	3.79	3.56	0.52	1.21	0.55	0.08	37.33
	8	7.75	4.03	1.92	2.50	1.03	0.33	159.44
	∞	8.40	5.48	4.54	2.66	1.48	0.55	215.66
3	2	0.79	3.22	0.15	0.21	0.50	0.01	1.73
	3	2.59	3.53	0.48	0.77	0.55	0.04	16.97
	8	5.49	4.63	2.31	1.63	0.85	0.20	78.99
	∞	3.54	3.23	0.59	1.14	0.68	0.09	36.69
6	2	0.79	3.21	0.14	0.21	0.49	0.01	1.69
	3	2.41	3.39	0.39	0.72	0.52	0.03	14.97
	8	5.31	4.22	1.82	1.63	0.87	0.19	78.88
	∞	2.00	3.09	0.23	0.64	0.49	0.03	12.81
10	2	0.79	3.20	0.14	0.21	0.50	0.01	1.69
	3	2.34	3.41	0.37	0.70	0.53	0.03	13.91
	8	4.45	4.10	1.50	1.31	0.75	0.13	50.85
	∞	1.90	3.10	0.21	0.61	0.48	0.03	11.17

Table 4.10: Transformation of guards by Stochastic Force (guards-based) on the map *potholes*

m	p	AVG1 $\times 10^{-2}$	MAX1 $\times 10^{-1}$	VAR1 $\times 10^{-3}$	AVG2 $\times 10^{-2}$	MAX2 $\times 10^{-1}$	VAR2 $\times 10^{-3}$	S $\times 10^{6}$
2	2	2.42	4.27	0.80	0.72	1.04	0.05	17.25
	3	4.46	4.61	1.19	1.51	1.12	0.14	62.09
	8	8.06	4.67	2.70	2.80	1.15	0.45	206.84
	∞	9.48	9.09	9.06	3.18	1.98	0.97	349.90
3	2	2.29	3.55	0.62	0.67	0.80	0.04	14.23
	3	3.50	3.64	1.02	1.09	0.90	0.09	34.26
	8	6.65	5.35	2.83	2.19	1.20	0.33	136.81
	∞	3.75	4.33	1.07	1.26	1.10	0.13	47.82
6	2	2.23	3.65	0.58	0.65	0.82	0.04	12.96
	3	3.28	3.69	0.92	1.01	0.84	0.07	29.95
	8	5.89	5.38	2.42	1.92	1.06	0.26	107.77
	∞	2.16	3.33	0.45	0.71	0.78	0.04	16.01
10	2	2.23	3.67	0.58	0.65	0.82	0.04	12.96
	3	3.22	3.71	0.88	1.00	0.84	0.07	28.98
	8	5.98	5.28	2.43	1.96	1.09	0.28	112.55
	∞	1.94	3.29	0.39	0.64	0.77	0.04	13.14

Table 4.11: Transformation of guards by Stochastic Force (guards-based) on the map *var_density*

m	p	AVG1 $\times 10^{-2}$	MAX1 $\times 10^{-1}$	VAR1 $\times 10^{-3}$	AVG2 $\times 10^{-2}$	MAX2 $\times 10^{-1}$	VAR2 $\times 10^{-3}$	S $\times 10^{6}$
2	2	8.83	47.97	15.25	3.31	2.42	1.00	677.64
3	2	7.59	862.51	394.05	2.69	2.59	0.54	408.17
6	2	5.75	86.97	12.10	2.09	1.01	0.27	228.09
10	2	5.83	111.85	26.38	1.97	0.99	0.25	206.28

Table 4.12: Transformation of environment by SMACOF (environment-based) on the map *jari*

m	p	AVG1 $\times 10^{-2}$	MAX1 $\times 10^{-1}$	VAR1 $\times 10^{-3}$	AVG2 $\times 10^{-2}$	MAX2 $\times 10^{-1}$	VAR2 $\times 10^{-3}$	S $\times 10^{6}$
2	2	5.08	179.01	97.28	1.34	4.86	1.34	140.12
3	2	2.52	10.07	2.82	0.57	0.82	0.05	7.06
6	2	2.55	10.17	2.35	0.55	0.73	0.04	6.30
10	2	2.56	10.16	2.43	0.55	0.73	0.04	6.28

Table 4.13: Transformation of environment by SMACOF (environment-based) on the map *pot-holes*

m	p	AVG1 $\times 10^{-2}$	MAX1 $\times 10^{-1}$	VAR1 $\times 10^{-3}$	AVG2 $\times 10^{-2}$	MAX2 $\times 10^{-1}$	VAR2 $\times 10^{-3}$	S $\times 10^{6}$
2	2	7.59	377.14	132.73	1.96	7.99	2.21	836.29
3	2	2.92	11.25	1.93	0.63	1.13	0.03	23.55
6	2	2.88	10.39	2.16	0.58	0.82	0.03	19.16
10	2	2.90	10.09	2.23	0.58	0.81	0.03	18.83

Table 4.14: Transformation of environment by SMACOF (environment-based) on the map *var_density*

m	p	AVG1 $\times 10^{-2}$	MAX1 $\times 10^{-1}$	VAR1 $\times 10^{-3}$	AVG2 $\times 10^{-2}$	MAX2 $\times 10^{-1}$	VAR2 $\times 10^{-3}$	S $\times 10^{6}$
2	2	7.04	9.29	7.20	2.59	1.93	0.54	202.12
3	2	6.40	16.47	5.11	2.38	1.88	0.42	164.77
6	2	6.05	8.62	3.77	2.22	1.84	0.36	143.06
10	2	5.97	8.36	3.74	2.19	1.83	0.36	140.83

Table 4.15: Transformation of guards by SMACOF (environment-based) on the map *jari*

m	p	AVG1 $\times 10^{-2}$	MAX1 $\times 10^{-1}$	VAR1 $\times 10^{-3}$	AVG2 $\times 10^{-2}$	MAX2 $\times 10^{-1}$	VAR2 $\times 10^{-3}$	S $\times 10^{6}$
2	2	10.19	92.59	72.96	2.73	3.96	2.68	617.23
3	2	5.52	53.85	26.96	1.15	2.20	0.40	89.34
6	2	5.54	53.95	27.02	1.15	2.19	0.40	89.37
10	2	5.54	53.90	27.01	1.15	2.19	0.40	89.38

Table 4.16: Transformation of guards by SMACOF (environment-based) on the map *potholes*

m	p	AVG1 $\times 10^{-2}$	MAX1 $\times 10^{-1}$	VAR1 $\times 10^{-3}$	AVG2 $\times 10^{-2}$	MAX2 $\times 10^{-1}$	VAR2 $\times 10^{-3}$	S $\times 10^{6}$
2	2	17.42	94.96	134.57	5.54	6.81	8.03	1931.51
3	2	3.23	7.58	1.43	0.91	1.05	0.06	23.79
6	2	3.23	8.38	1.62	0.86	0.90	0.05	20.97
10	2	3.24	8.27	1.67	0.85	0.90	0.05	20.70

Table 4.17: Transformation of guards by SMACOF (environment-based) on the map *var_density*

m	p	AVG1 $\times 10^{-2}$	MAX1 $\times 10^{-1}$	VAR1 $\times 10^{-3}$	AVG2 $\times 10^{-2}$	MAX2 $\times 10^{-1}$	VAR2 $\times 10^{-3}$	S $\times 10^{6}$
2	2	6.52	9.20	7.33	2.32	1.74	0.47	167.70
3	2	5.63	24.11	4.67	2.08	1.29	0.34	129.38
6	2	5.10	10.43	2.85	1.91	1.08	0.28	108.42
10	2	5.04	11.26	2.81	1.88	1.06	0.28	106.04

Table 4.18: Transformation of guards by SMACOF (guards-based) on the map *jari*

m	p	AVG1 $\times 10^{-2}$	MAX1 $\times 10^{-1}$	VAR1 $\times 10^{-3}$	AVG2 $\times 10^{-2}$	MAX2 $\times 10^{-1}$	VAR2 $\times 10^{-3}$	S $\times 10^{6}$
2	2	0.82	3.63	0.19	0.21	0.50	0.01	1.75
3	2	0.85	4.20	0.20	0.21	0.41	0.01	1.60
6	2	0.87	4.40	0.22	0.21	0.39	0.00	1.51
10	2	0.89	4.48	0.22	0.21	0.39	0.00	1.49

Table 4.19: Transformation of guards by SMACOF (guards-based) on the map *potholes*

m	p	AVG1 $\times 10^{-2}$	MAX1 $\times 10^{-1}$	VAR1 $\times 10^{-3}$	AVG2 $\times 10^{-2}$	MAX2 $\times 10^{-1}$	VAR2 $\times 10^{-3}$	S $\times 10^{6}$
2	2	2.53	5.50	0.98	0.71	0.94	0.04	15.78
3	2	2.45	6.39	0.94	0.65	0.72	0.03	12.75
6	2	2.43	6.96	0.96	0.62	0.68	0.03	11.09
10	2	2.45	7.01	0.99	0.62	0.68	0.03	10.99

Table 4.20: Transformation of guards by SMACOF (guards-based) on the map *var_density*

		jari			*potholes*			*var_density*		
m	p	SOM	CAN	ORC	SOM	CAN	ORC	SOM	CAN	ORC
6	2	35309	32962	33147	26162	26891	26400	24537	24059	24831
	∞	36466	33943	34365	27349	26298	26809	25927	25030	25481
10	2	35073	32775	33027	26144	26425	26395	24663	23993	24730
	∞	36380	33891	34041	27446	27769	26800	26099	27283	25262

Table 4.21: SOM comparison using environment-based Stochastic Force

		jari			*potholes*			*var_density*		
m	p	SOM	CAN	ORC	SOM	CAN	ORC	SOM	CAN	ORC
6	2	35039	32623	32996	24599	24073	24859	24852	23875	24613
	∞	36465	34454	34338	24807	35343	24929	25626	26670	24999
10	2	35251	32413	32694	24622	23979	24773	24651	23934	24610
	∞	37713	34284	34370	24928	42130	24953	26003	33585	25262

Table 4.22: SOM comparison using guards-based Stochastic Force

		jari			*potholes*			*var_density*		
m	p	SOM	CAN	ORC	SOM	CAN	ORC	SOM	CAN	ORC
6	2	36500	34459	34358	26318	26825	26648	25026	24871	24843
10	2	36117	34064	34044	26486	26639	26760	25080	24342	24708

Table 4.23: SOM comparison using environment-based SMACOF

		jari			*potholes*			*var_density*		
m	p	SOM	CAN	ORC	SOM	CAN	ORC	SOM	CAN	ORC
6	2	37048	34230	34257	24761	24734	24888	25152	25043	24614
10	2	36877	33880	34007	24715	24352	24983	25304	24371	24719

Table 4.24: SOM comparison using guards-based SMACOF

Chapter 5

Conclusion

A method for solving the travelling salesman problem in a polygonal domain was presented in the thesis. It is based on a transformation of the polygonal domain into a metric space using the multidimensional scaling algorithms.

The MDS methods were used for application of the SOM algorithms for the Euclidean TSP in a polygonal domain. Different MDS methods with various parameters were implemented and tested. The SOM algorithms used in this experiment were designed for the two-dimensional Euclidean spaces $< R^2, l_2 >$, but they were applied in more general $< R^m, l_p >$.

The experiments have shown that the developed approach works. However, since the algorithms were used in an nontraditional way, it is safe to conclude that their performance is not optimal, and it can be improved.

Various parameters (number of dimensions, norm, guards-based and environment-based approach) were tested, but it did not become clear what parameters are the most suitable, although some of the tested parameters (l_3, l_8) were excluded. Since a number of variations have shown promising results, several algorithm modifications can be developed based on this approach.

Currently, guards transformation leads to a poor local performance (for example, small loops emerge), therefore developing a better method of the local guards positioning (especially for l_∞ norm) may improve the produced results. Both direct and indirect methods have this problem. Development of a new SOM algorithm that is more apt for l_∞ and various numbers of dimensions could also greatly influence the quality of the solution. It is also necessary to optimise the termination of Stochastic Force to improve its speed. Other multidimensional scaling algorithms may be tested, especially Glimmer [15], which uses stochastic force as a module and has a GPU implementation, allowing parallel computations.

Bibliography

[1] Teuvo Kohonen. Self-organized formation of topologically correct feature maps. *Biological Cybernetics*, 43(1):59–69, 1982.

[2] Samerkae Somhom, Abdolhamid Modares, and Takao Enkawa. A self-organising model for the travelling salesman problem. *Journal of the Operational Research Society*, pages 919–928, 1997.

[3] EM Cochrane and JE Beasley. The co-adaptive neural network approach to the euclidean travelling salesman problem. *Neural Networks*, 16(10):1499–1525, 2003.

[4] Junying Zhang, Xuerong Feng, Bin Zhou, and Dechang Ren. An overall-regional competitive self-organizing map neural network for the euclidean traveling salesman problem. *Neurocomputing*, 89:1–11, 2012.

[5] Keld Helsgaun. An effective implementation of the lin–kernighan traveling salesman heuristic. *European Journal of Operational Research*, 126(1):106–130, 2000.

[6] Licheng Jiao and Lei Wang. A novel genetic algorithm based on immunity. *Systems, Man and Cybernetics, Part A: Systems and Humans, IEEE Transactions on*, 30(5):552–561, 2000.

[7] Marco Dorigo and Luca Maria Gambardella. Ant colony system: a cooperative learning approach to the traveling salesman problem. *Evolutionary Computation, IEEE Transactions on*, 1(1):53–66, 1997.

[8] Jan Faigl, Miroslav Kulich, Vojtěch Vonásek, and Libor Přeučil. An application of the self-organizing map in the non-euclidean traveling salesman problem. *Neurocomputing*, 74(5):671–679, 2011.

[9] Jan Faigl. On the performance of self-organizing maps for the non-euclidean traveling salesman problem in the polygonal domain. *Information Sciences*, 181(19):4214–4229, 2011.

[10] Richard Durbin and David Willshaw. An analogue approach to the travelling salesman problem using an elastic net method. *Nature*, (326):689–91, 1987.

[11] Donald B Johnson. Efficient algorithms for shortest paths in sparse networks. *Journal of the ACM (JACM)*, 24(1):1–13, 1977.

[12] Ingwer Borg and Patrick JF Groenen. *Modern multidimensional scaling: Theory and applications*. Springer Science & Business Media, 2005.

[13] Asi Elad and Ron Kimmel. On bending invariant signatures for surfaces. *Pattern Analysis and Machine Intelligence, IEEE Transactions on*, 25(10):1285–1295, 2003.

[14] Matthew Chalmers. A linear iteration time layout algorithm for visualising high-dimensional data. In *Visualization'96. Proceedings.*, pages 127–131. IEEE, 1996.

[15] Stephen Ingram, Tamara Munzner, and Marc Olano. Glimmer: Multilevel mds on the gpu. *Visualization and Computer Graphics, IEEE Transactions on*, 15(2):249–261, 2009.

Appendix

CD Content

In table 5.1 are listed names of all root directories on CD

Directory name	**Description**
maps	Maps used for testing
sompd	Source code of the implementation

Table 5.1: CD Content